Journal of Applied Electrochemistry **31**: 1185–1193, 2001.

Electrochemical reduction of nitrate in weakly alkaline solutions

K. BOUZEK, M. PAIDAR, A. SADÍLKOVÁ and H. BERGMANN*
*Department of Inorganic Technology, Institute of Chemical Technology, Technická 5, 16628 Prague 6, Czech Republic (*Anhalt University of Applied Sciences, Bernburger Strasse 55, D-06366 Köthen, Germany)*

Received 22 December 2000; accepted in revised form 3 July 2001

Key words: cyclic voltammetry, electrocatalytic activity, nitrate reduction, rotating ring disc electrode, weakly alkaline

Abstract

The electrocatalytic activity of several materials for the nitrate reduction reaction was studied by cyclic voltammetry on a rotating ring disc electrode in solutions with different concentrations of sodium bicarbonate. Copper exhibited highest catalytic activity among the materials studied. Nitrate reduction on copper was characterized by two cathodic shoulders on the polarization curve in the potential region of the commencement of hydrogen evolution. In this potential range an anodic current response was observed on the Pt ring electrode identified as nitrite to nitrate oxidation. This indicates that nitrite is an intermediate product during nitrate reduction. These conclusions were verified by batch electrolysis using a plate electrode electrochemical cell. Copper and nickel, materials representing the opposite ends of the electrocatalytic activity spectra, were used in batch electrolysis testing.

1. Introduction

The electrochemical reduction of nitrates (NO_3^-) represents an attractive alternative method for the reduction of pollution of drinking water by this anion. The heterogeneous nature of the electrochemical processes calls, however, for a complementary method providing pre-concentration of the NO_3^- ions in the process water suitable for electrochemical treatment. Ionic exchange was chosen as the most suitable method. This is mainly because of its high selectivity to NO_3^- ions and its economic operation. $NaHCO_3$ was identified as a suitable regenerating agent for ion exchanger saturated by NO_3^-. HCO_3^- ions represent an important constituent of drinking water and their addition is more desirable than chloride whose concentration in drinking water is limited [1]. By combining the ion exchange process with the subsequent electrochemical treatment (NO_3^- reduction) of the spent solution it is possible to reuse it in a closed cycle.

The electrochemical reduction of NO_3^- was first studied mainly in acidic solutions [2–5]. The highest electrocatalytic activity was observed for platinum metals [2–4]. It was found that alloying two metals [3] and/or their modification with a monolayer of germanium [4] leads to increased catalytic activity. This phenomenon was explained by bifunctional catalysis.

NO_3^- reduction was also studied using a polycrystalline gold electrode in electrolytes of different pH [5]. It was found that hydrogen adsorbed on the cathode surface inhibits NO_3^- reduction (most apparent at acidic pH). This is consistent with results from [2–4].

Later attention focused on nitrate reduction in strongly alkaline solutions (1 to 3 M NaOH). The main reason was the need to find a suitable way of handling large amounts of high-level wastes containing NO_3^- and NO_2^- originating from processing nuclear materials [6, 7]. Cd and Pb cathodes were identified as the most efficient [6]. Because of their toxicity, however, these materials can hardly be used for drinking water treatment. Ni and Cu cathodes are singled out as a more suitable option. According to Bockris and Kim [7, 8], who studied the behaviour of Ni, Fe and Pb electrodes in concentrated NaOH solution, NO_3^- reduction was again suppressed in the potential region of hydrogen evolution.

Li et al. [9] studied the application of Pt and Ni electrodes for processing alkaline solutions containing NO_3^- ions at elevated temperatures. They observed that, by using a platinised Ni electrode, NO_3^- is reduced with high efficiency. The reaction kinetics was controlled by unspecified electrode surface phenomena. A positive influence of Pb adatoms on the Au cathode catalytic activity was observed in alkaline solutions [10].

A cyclic voltammetric study of the behaviour of Ag, Cu and semiconducting $CuInSe_2$ electrodes in alkaline NO_3^- solutions was made by Cattarin [11], who reported the following main conclusions. Whereas on the Ag electrode the NO_3^- ions are reduced to nitrite (NO_2^-), on the Cu cathode the final product is ammonia (NH_3). The

Ag electrode shows one cathodic peak (see letter). After irradiation the semiconducting cathode ($CuInSe_2$) shows a shift in electrode potential corresponding to a rise in the cathodic current to an approximately 400 mV less cathodic value when compared to the electrode in dark. However, because of the low electrocatalytic activity of this material, even at the illuminated cathode, nitrate reduction is overlapped by hydrogen evolution.

A similar study was also performed using graphite, either pure or modified with the phthalocyanides of different metals [12]. NH_3 was found to be the main reduction product.

The present work deals with $NaHCO_3$ solutions suitable for the regeneration of the ion exchanger used in drinking water treatment. This solution differs substantially from the electrolytes referred to in the literature to date (except our previous study [13]). It is known that electrochemical NO_3^- reduction is sensitive to the composition of the solution and especially to its pH. Therefore, conclusions made in previous studies have to be verified for this particular electrolyte solution. On the basis of a literature search the following materials were chosen: Cu, Ni, graphite and Pt. The aim of this study is to compare the electrocatalytic activity of these materials for NO_3^- reduction in weakly alkaline media with results published for strongly alkaline electrolytes and to identify the cathode material most suitable for the construction of an electrochemical cell for the NO_3^- reduction process.

2. Experimental details

2.1. *Apparatus*

The cyclic voltammetric curves were measured using a PINE AFMSRX electrode rotator and a PINE AFCBP1 bipotentiostat controlled by a personal computer equipped with PineChem 2.7.5. software. The dimensions of the ring-disc electrode were as follows: disc radius 3 mm, inner radius of the ring 3.75 mm, ring outer radius 4.25 mm and whole assembly radius 7.50 mm.

A plate electrode cell in a recirculation mode was used for the batch electrolysis. It consisted of three activated Ti anodes and two cathodes. The active surface area of the cathodes was 1000 cm^2. A detailed diagram of the cell is given in [13].

A saturated calomel electrode (SCE) was used and all potentials refer to this electrode.

2.2. *Chemicals*

If not otherwise stated in the text an artificial electrolyte simulating spent solution after regeneration of the ion exchanger was used. Its composition was as follows (in g dm^{-3}): $NaHCO_3$ 84, NaCl 0.4 and Na_2SO_4 0.4. Blank experiments without addition of NO_2^- or NO_3^- to the electrolyte were performed. Tests with NO_3^- and NO_2^- in these electrolytes featured the addition of 1 g dm^{-3} of NO_3^- in the form of $NaNO_3$ or 1 g dm^{-3} NO_2^- in the form of $NaNO_2$.

2.3. *Analytical methods*

Determination of NO_3^- content was based on light absorption at 210 nm [14]; NO_2^- was allowed to react with sulfanilic acid and α-naphtol in acidic solution yielding an orange-coloured azo dyestuff with absorption maximum at 476 nm [14]. NH_3 was allowed to react with the Nessler agent and determined spectrophotometrically at 380 nm [14]. Cu ion content was determined by atomic absorption spectroscopy.

3. Results

3.1. *Copper cathode*

On Cu the voltammetric curves were measured in the potential range from −0.2 to −1.6 V. At the beginning of each experiment the electrode was polarized for 30 s at a potential of 0.0 V. At this potential slow anodic dissolution of the Cu electrode takes place. This ensures reproducibility of the electrode surface at the beginning of each experiment.

The polarization curve of the Cu electrode in electrolytes with and without NO_3^- addition are shown in Figure 1. The addition of NO_3^- ions results in the appearance of the two current waves in the potential region of hydrogen evolution. Overlap of the current corresponding to NO_3^- reduction by the current for hydrogen evolution complicates a more detailed study of the reaction. Therefore the hydrogen evolution background current (blank experiment) was subtracted from the polarization curve for NO_3^- addition. The resulting curve is shown in Figure 2. Two cathodic current peaks result from the subtraction. They are denoted in Figure 2 as peaks $I_{(Cu)}$ and $II_{(Cu)}$. Peak $I_{(Cu)}$ is partially overlapped by peak $II_{(Cu)}$ and appears as a shoulder on its rising part. The good reproducibility of these peaks indicates that they correspond to the NO_3^- reduction reaction. To provide more satisfactory evidence of their origin a current response on the Pt ring electrode was followed. A current peak was observed at potentials of 0.95 V and higher. This is shown for the ring electrode potential of 1.0 V in Figure 2. The anodic response current peak coincides with the reduction peak $I_{(Cu)}$ on the disc electrode. These two independent observations show that the cathodic current peak observed on the Cu disc electrode originates from NO_3^- reduction.

With respect to its potential the current response on the ring electrode corresponds to the oxidation of the intermediate or final products of NO_3^- reduction on the disc electrode. As discussed in the theoretical part of this study, one of the final products most often referred to is NH_3 [11, 12]. On the polarization curves of the Pt

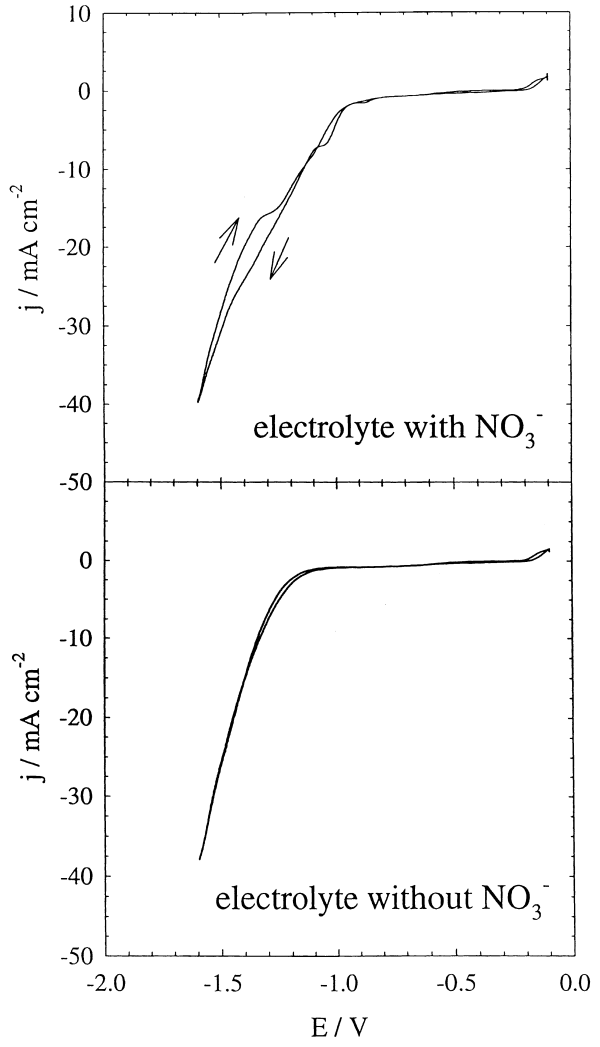

Fig. 1. Cyclic voltammetric curves on the Cu RDE electrode in the electrolyte with and without NO_3^- addition, electrode rotation rate 20 Hz, potential scan rate 10 mV s^{-1}. Arrows indicate the direction of the course of the polarization curve.

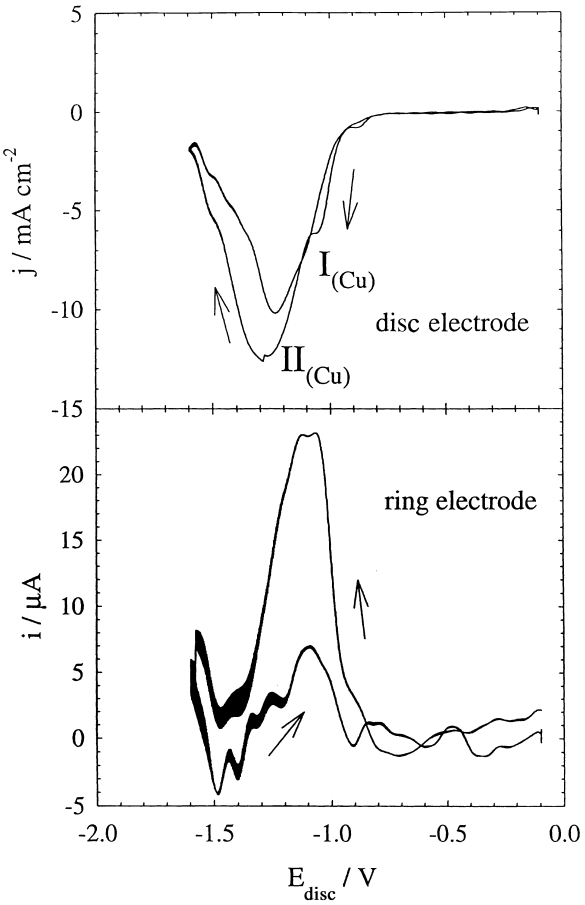

Fig. 2. Cyclic voltammetric curve on the Cu RDE electrode and Pt ring electrode in the electrolyte containing NO_3^- after subtraction of the curve for blank electrolyte, electrode rotation rate 20 Hz, potential scan rate 10 mV s^{-1}, potential of ring electrode 1.0 V. Arrows indicate the direction of the course of the polarization curve.

rotating disc electrode (RDE) in electrolytes with an addition of 0.4 g dm^{-3} of NH_3 no current response corresponding to NH_3 oxidation was observed. Moreover, on the polarization curve measured for the electrolyte containing NH_3 a deterioration in the oxygen evolution reaction was evident (not shown here).

In the next step the reduction of NO_2^- was studied. The resulting polarization curve with subtracted hydrogen evolution background is shown together with the current response on the Pt ring electrode in Figure 3. On the Pt ring electrode at 1.0 V NO_2^- is oxidized continuously to NO_3^-. An initial current increase (E_{disc} = −1.3 V), followed by a decrease on the ring electrode, corresponds to the NO_2^- reduction current wave on the Cu disc electrode.

The decrease in current of the ring electrode in the potential region of the cathodic current wave of the disc indicates that the electrolyte coming to the ring electrode was depleted by the electroactive species, that is, NO_2^- by the reaction taking place on the disc electrode in this potential region. A distinct anodic current peak corresponding to NO_2^- oxidation was observed at the Pt disc electrode at 1.0 V shown in Figure 4. This proves the origin of the anodic current response shown in Figure 2.

The NO_2^- reduction on the Cu disc electrode shown in Figure 3 exhibits the following differences in comparison to the reduction of NO_3^- (Figure 2). The current density of the wave is well above the NO_3^- reduction peak, the curve does not exhibit peak $I_{(Cu)}$ and, finally, it does not exhibit a strong decrease at potentials more cathodic than −1.3 V.

As shown previously [13], the addition of Cu ions to the solutions treated enhances the electrolysis efficiency. An experiment was performed with the addition of 2 g dm^{-3} of $CuCO_3 \cdot Cu(OH)_2 \cdot 3H_2O$. The concentration of Cu ions in the solution was determined at 5 mg dm^{-3}. The remaining salt is present in solid form. The curve after subtraction of the background current is shown, together with the ring current response, in Figure 5. The addition of Cu ions resulted in an increase in peak current density of the NO_3^- reduction, as well as in an increase in current response on the Pt ring electrode. As is apparent from the disc electrode polarization curve, a current peak is initiated at a

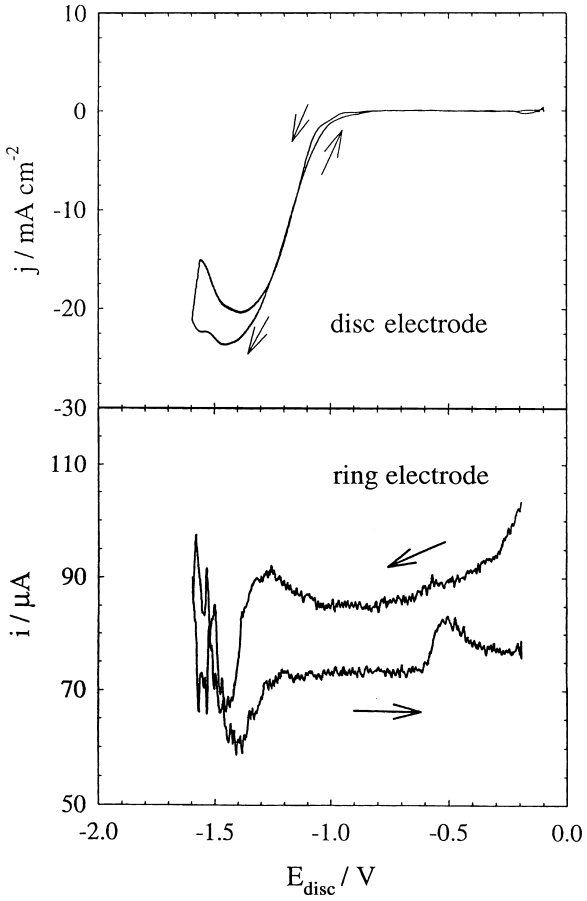

Fig. 3. Cyclic voltammetric curve on the Cu RDE electrode and Pt ring electrode in the electrolyte containing NO_2^- after subtraction of the curve for blank electrolyte, electrode rotation rate 20 Hz, potential scan rate 10 mV s^{-1}, potential of ring electrode 1.0 V. Arrows indicate the direction of the course of the polarization curve.

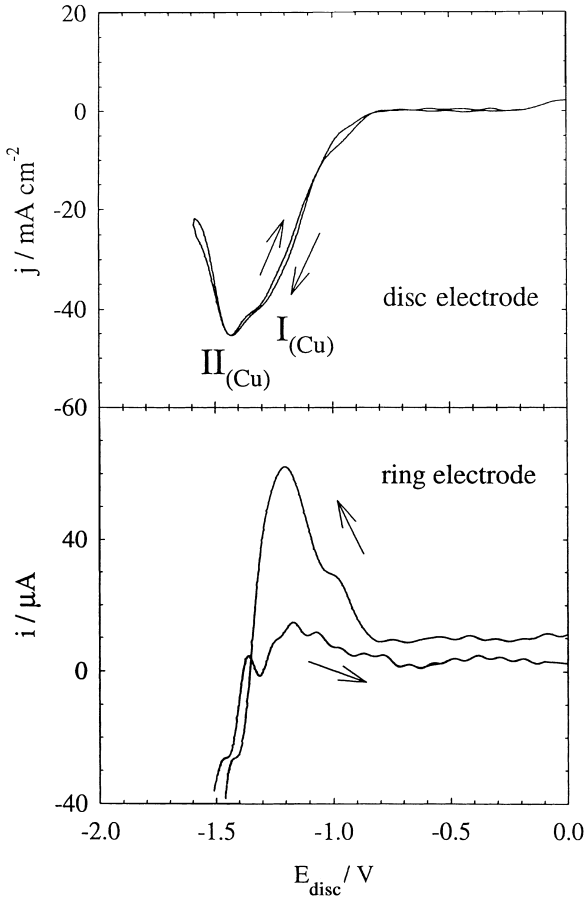

Fig. 5. Cyclic voltammetric curve on the Cu RDE electrode and Pt ring electrode in the electrolyte containing NO_3^- after subtraction of the curve for blank electrolyte, both electrolytes contain addition of Cu ions, electrode rotation rate 20 Hz, potential scan rate 10 mV s^{-1}, potential of ring electrode 1.0 V. Arrows indicate the direction of the course of the polarization curve.

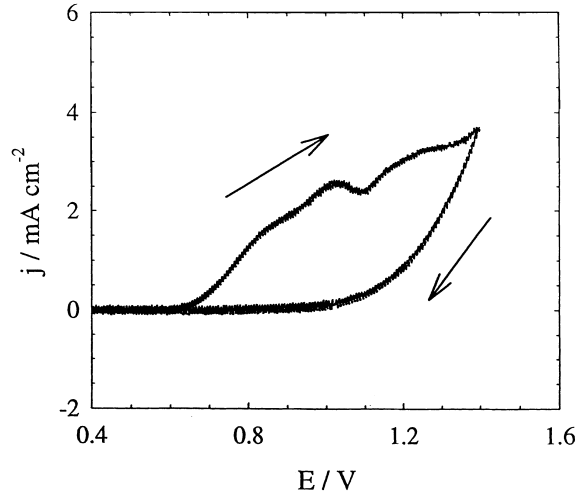

Fig. 4. Cyclic voltammetric curve on the Pt RDE electrode in the electrolyte containing NO_2^- after subtraction of the curve for blank electrolyte, electrode rotation rate 20 Hz, potential scan rate 10 mV s^{-1}. Arrows indicate the direction of the course of the polarization curve.

potential similar to that observed for the Cu disc electrode without addition of Cu ions. In the case of added Cu ions the rising part lasts longer and the potential of the peak is, therefore, more cathodic.

A series of experiments was performed with the ring electrode covered by a cathodically deposited Cu layer, which showed highest electrocatalytic activity at the conditions under study (as discussed later). The resulting current responses on the ring electrode at different potentials are shown in Figure 6. No current response was observed until the potential reached a value more cathodic than −0.9 V, that is, until the reduction of NO_3^- took place. At sufficiently cathodic potential a stable current corresponding to the NO_3^- reduction is observed. Its decrease coincides with the NO_3^- reduction at the disc electrode. A similar situation was also observed for the addition of NO_2^- and Cu ions to the electrolyte.

All experiments with a Cu electrode were performed using four types of electrolyte differing in the $NaHCO_3$ content (8 to 84 g dm^{-3}). It was observed that, with decreasing concentration of $NaHCO_3$, the current density of the peak $II_{(Cu)}$ gradually decreased and approached the value of peak $I_{(Cu)}$. This resulted in their slight separation.

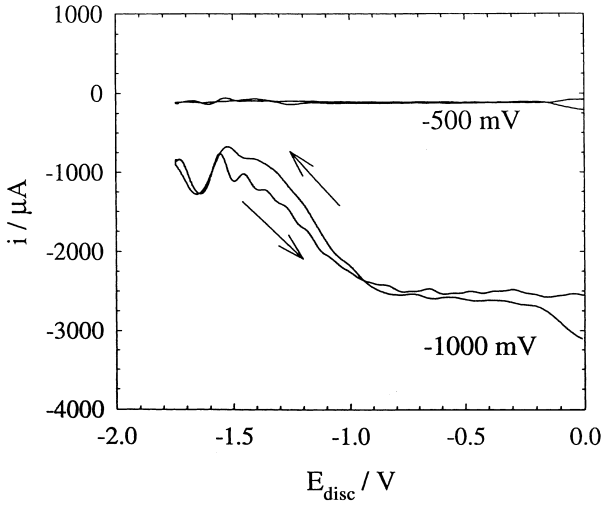

Fig. 6. Current response on the ring electrode covered by the cathodically deposited Cu layer for the Cu RDE in electrolyte containing NO_3^- after subtraction of the curve for blank electrolyte, potential of the ring electrode is indicated in the Figure, electrode rotation rate 20 Hz, potential of disc electrode scan rate 10 mV s^{-1}. Arrows indicate the direction of the course of the polarization curve.

3.2. *Nickel cathode*

In this case the electrode potential range from 1.6 to −1.6 V was studied and the electrode was polarized at the beginning of each experiment for 20 s at the anodic end of the potential scan rate. This assured reproducible electrode surface conditions at the beginning of each experiment.

Since no electrode reaction was identified in the anodic potential region, the part of the polarization curve ranging from 0.0 to −1.6 V is presented here. Surprisingly, lower electrocatalytic activity for NO_3^- reduction was observed, as shown in Figure 7. The cathodic current density on the subtracted polarization curve commences at more cathodic potential when compared to the Cu electrode. It is practically completely overlapped by the hydrogen evolution reaction. This fact corresponds with disturbances on the Ni disc, as well as on the Pt ring electrode held at a potential of 1.0 V, caused by the hydrogen gas bubbles. Despite this noise the course of the polarization curves was very reproducible. Other qualitative characteristics of the curve are similar to the copper electrode. Two cathodic peaks were identified, the less cathodic one being lower and partially overlapped by the second. The potential separation of these two peaks is more pronounced than in the case of Cu. The current densities of the peaks are lower when compared to Cu. The maximum for peak $II_{(Ni)}$ was not reached in the potential range under study. A further increase in the cathodic vertex potential resulted in disturbance of the signal by the hydrogen bubbles evolved.

NO_2^- reduction was also studied at the Ni cathode. Results indicated different behaviour for NO_2^- compared to NO_3^-. As shown in Figure 8, in this case one sharp cathodic current peak was reproducibly observed

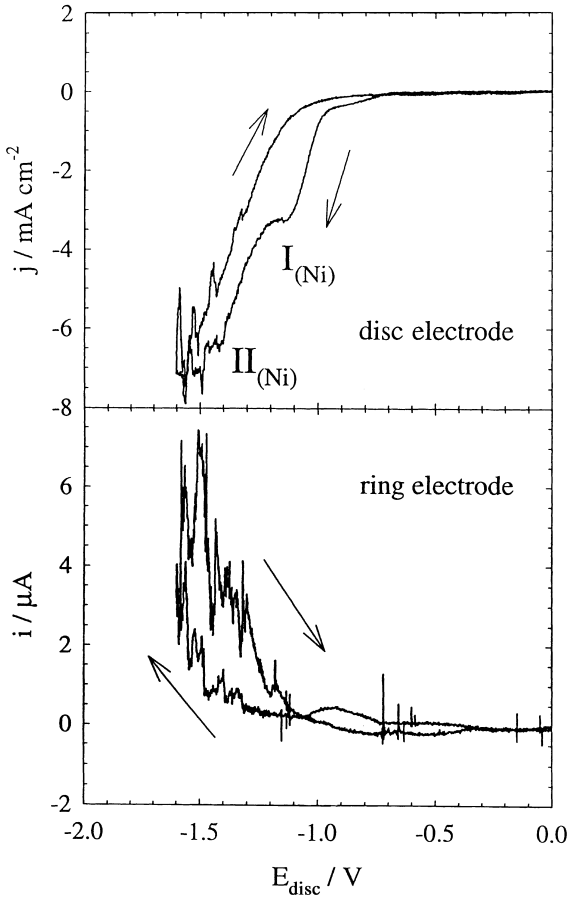

Fig. 7. Cyclic voltammetric curve on the Ni RDE electrode and Pt ring electrode in the electrolyte containing NO_3^- after subtraction of the curve for blank electrolyte, electrode rotation rate 20 Hz, potential scan rate 10 mV s^{-1}, potential of ring electrode 1.0 V. Arrows indicate the direction of the course of the polarization curve.

on the subtracted polarization curve during the cathodic potential scan. Its potential corresponds well with peak $I_{(Ni)}$ shown in Figure 7. The current response on the Pt ring electrode kept at a potential of 1.0 V shows a slight anodic current peak in the corresponding potential region. The subsequent decrease in current, corresponding to the reduction of NO_2^- on the disc electrode, however, does not take place. The possible explanation is that NO_2^- reduction products are oxidized on the Pt ring electrode causing an increase in the current response. The cathodic current densities on the disc electrode are low and, therefore, a response at the ring electrode is not well developed. During the reverse potential scan three cathodic current peaks appeared on the disc electrode. Their origin is not known. No corresponding current response was observed on the ring electrode.

3.3. *Graphite and platinum cathodes*

Experiments identical to those with the previous materials were also performed using graphite and platinum electrodes. Only weak signals of NO_3^- reduction were observed for both electrode materials. For NO_2^- reduction

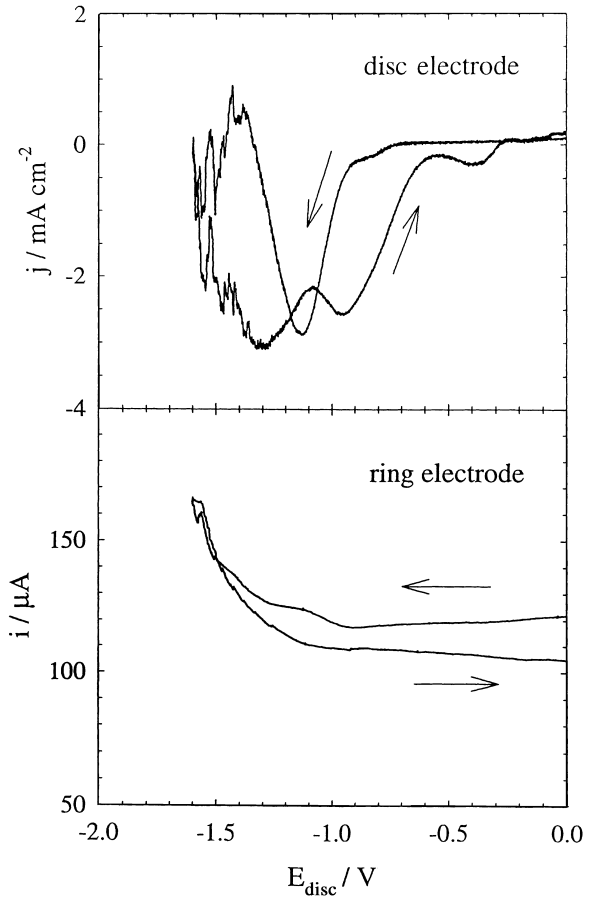

Fig. 8. Cyclic voltammetric curve on the Ni RDE electrode and Pt ring electrode in the electrolyte containing NO_2^- after subtraction of the curve for blank electrolyte, electrode rotation rate 20 Hz, potential scan rate 10 mV s^{-1}, potential of ring electrode 1.0 V. Arrows indicate the direction of the course of the polarization curve.

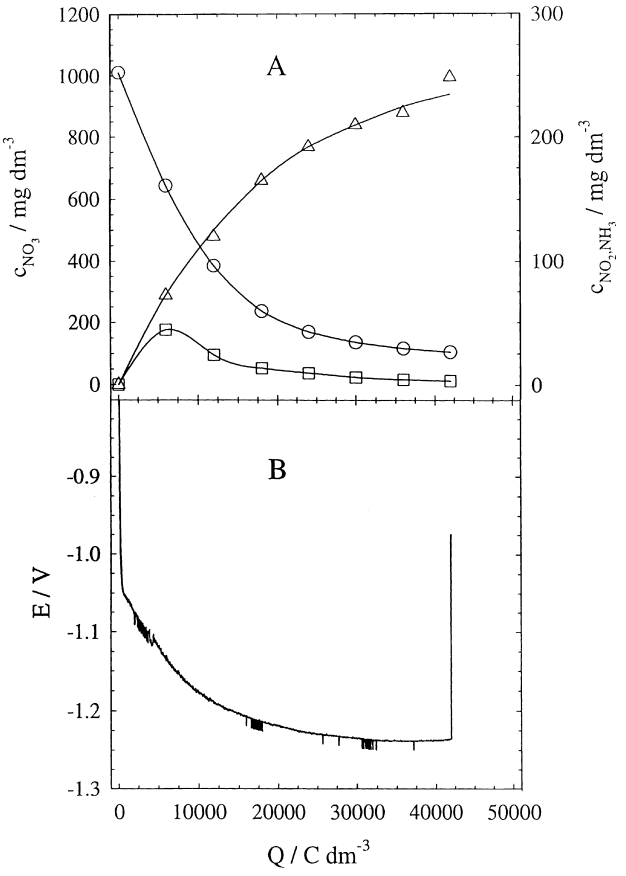

Fig. 9. Dependence of the (A) concentrations of nitrogen species in the solution and (B) Cu cathode potential on the electrical charge per volume of the electrolyte applied from the beginning of electrolysis, electrolyte with NO_3^-, temperature 20 °C, current density 4 mA cm^{-2}, concentration of: (◯) NO_3^-, (□) NO_2^- and (△) NH_3.

current densities on the cathodes were higher. According to its current response however, NO_2^- is reduced to a compound detectable on the Pt ring electrode. This indicates that the reduction mechanism of NO_3^- on these materials is different from that on Cu and the electrocatalytic activity for NO_3^- reduction is significantly lower.

3.4. *Batch electrolysis*

To verify the results obtained using cyclic voltammetry batch electrolysis tests were carried out using Cu and Ni cathodes. The results obtained are shown in Figures 9 and 10. The main results from the voltammetric experiments coincide with those of the batch electrolysis. With a Cu cathode the NO_3^- concentration drops to a value of 170 mg dm^{-3} within 24 000 C dm^{-3} with a current yield of 43%. For the Ni cathode under identical conditions the concentration was reduced only to 824 mg dm^{-3} with a yield of 7%.

It is also interesting to note the variation of cathode potential with electrolysis time. The potential against charge curve for the Cu electrode shows a distinct dependence on NO_3^- concentration. After the electrolysis has started the potential quickly approaches a value of about −1.05 V. This corresponds well with the region of NO_3^- reduction to NO_2^- as shown in Figure 2. After the mass-transfer limiting current density was exceeded, at this particular current density a few minutes after the start of electrolysis, the potential shifted to a more cathodic value. In contrast to this, the potential of the Ni cathode briefly reached a maximum after switching the current and decreased gradually (became more anodic). At all times, however, the potential remained in the region of the hydrogen evolution reaction.

Potentiostatic electrolysis was performed in order to identify the main NO_3^- reduction product at different electrode potentials. The results are summarised in Figure 11. It can be seen that at a potential of −0.85 V the reduction proceeds primarily to the NO_2^- stage with very little NH_3 formed. Significant reduction to NH_3 is first apparent at −0.90 V with quantitative reduction of NO_2^- to NH_3 first reached at a cathode potential more cathodic than −1.00 V. If the potential, however, exceeds −1.2 V, electrolysis efficiency starts to decrease. This corresponds to the potential where the peak maximum is reached (see Figure 2) and where inhibition of NO_3^- reduction by the hydrogen evolved takes place.

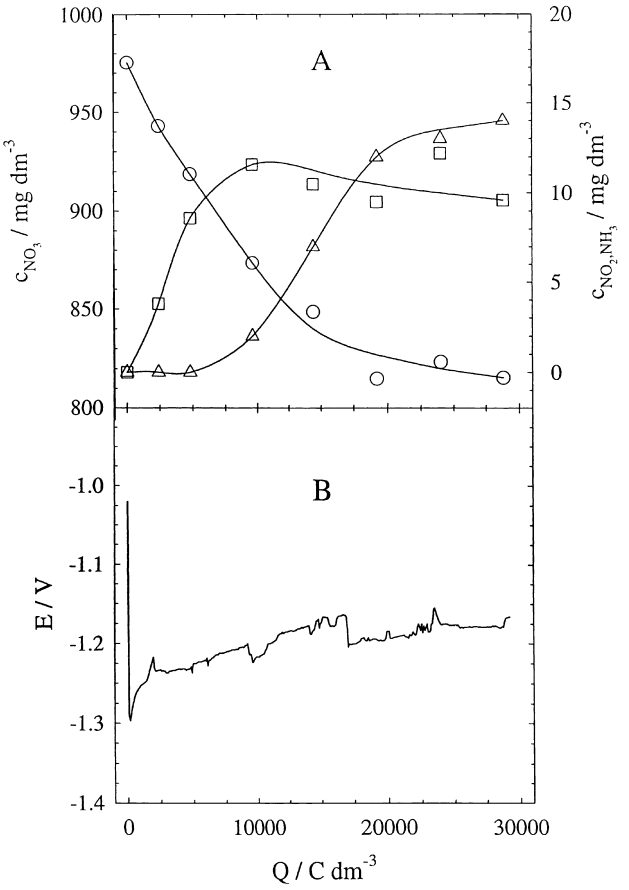

Fig. 10. Dependence of the (A) concentrations of nitrogen species in the solution and (B) Ni cathode potential on the electrical charge per volume of the electrolyte applied from the beginning of electrolysis, electrolyte with NO_3^-, temperature 20 °C, current density 4 mA cm^{-2}, concentration of: (○) NO_3^-, (□) NO_2^- and (△) NH_3.

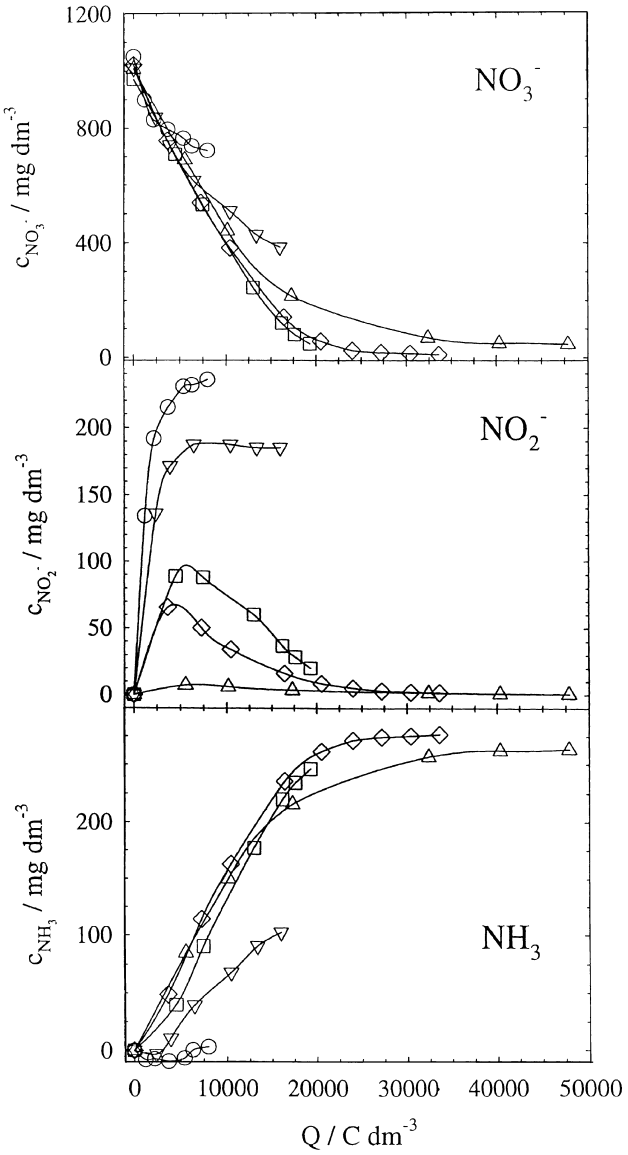

Fig. 11. Dependence of the NO_3^-, NO_2^- and NH_3 concentration in the solution on the electrical charge per volume of the electrolyte applied from the beginning of electrolysis, temperature 20 °C, cathode potential: (○) −0.85 V, (△) −0.90 V, (□) −1.00 V, (◇) −1.10 V and (△) −1.20 V.

4. Discussion

The highest catalytic activity for nitrate reduction among the materials tested occurred with Cu. Therefore mainly results obtained for this material will be discussed.

One interesting feature is that on the Cu polarization curve for NO_3^- reduction a current peak appears, instead of a limiting current, as expected for the mass-transfer controlled reaction on the rotating disc electrode and the slow potential scan rate (Figure 2). This can be explained by the inhibition of the NO_3^- reduction by the hydrogen adsorbed on the Cu surface as discussed in the introduction [2–5]. This factor becomes important in the potential region of intensive hydrogen evolution. Such behaviour indicates that the NO_3^- reduction process is only partially controlled by mass transfer. This was verified by a Koutecký–Levich analysis of the results for different RDE rotation rates. The kinetic current density value of 13 mA cm^{-2} was found by extrapolation of the dependence of the inversed current density value of the cathodic peak on $\omega^{-1/2}$ (where ω is an angular rotation rate) to infinitely fast rotation. In the case of Cu ions addition the kinetic current density increased to 110 mA cm^{-2}. The kinetic current density cannot be exceeded even when the mass transfer limit is above this value. Exceeding the kinetic current density results in the commencement of hydrogen evolution and subsequent inhibition of NO_3^- reduction. The higher kinetic current density value observed for Cu addition explains the higher current efficiency of NO_3^- reduction found at higher current densities [13].

The mechanism of nitrate reduction in weakly alkaline solutions has not been studied so far. The subtracted polarization curve given in Figure 2 shows two overlapping cathodic peaks. This is in general agreement with the curves presented by Cattarin [11]. The main differences are the clear separation of the cathodic current peaks corresponding to the NO_3^- reduction and hydrogen evolution reaction and splitting of the peak $II_{(cu)}$ into two individual peaks apparent on the curves presented by Cattarin. The separation of the hydrogen

evolution is caused by the higher pH of the solution used in [11] (1 M NaOH) and the subsequent shift of this reaction to more cathodic potentials. The potential of the current peaks is close in both solutions. The splitting indicates changes in the kinetics of the individual electrode reactions (see letter).

The absence of cathodic peak $I_{(Cu)}$ on the polarization curve obtained for the solution containing NO_2^- ions (Figure 3) confirms that this peak corresponds to NO_3^- reduction to NO_2^-. This is further verified by the current response observed on the Pt ring electrode indicating that, in the potential region of the current peak $I_{(Cu)}$, NO_2^- is produced on the disc electrode. This means that the NO_3^- reduction proceeds as a first step to NO_2^-, as observed during batch electrolysis with Cu. Here in the potential range of peak $I_{(Cu)}$ only, NO_2^- is the sole or main reaction product. With the commencement of current peak $II_{(Cu)}$ reduction proceeds to an increasing extent to NH_3 as the final product (Figure 11).

According to the batch electrolysis results the current peak $II_{(Cu)}$ corresponds to the so far unspecified series of reactions leading from NO_2^- to NH_3. This is also indicated by the current response on the Pt ring electrode shown in Figure 3 and discussed below. The current increase with the peak potential of -1.3 V clearly indicates one of the complex reaction mechanism steps taking place in this potential region.

The polarization curve of the NO_2^- reduction reaction does not exhibit such a distinct current peak. Its course is much more like that of a limiting current and its current density is higher when compared to NO_3^- reduction. This indicates that the process is less sensitive to inhibition by hydrogen atoms.

A study of the current response on the ring electrode covered by the cathodically deposited Cu (Figure 6) showed only a decrease in current response in the potential region where NO_3^- is reduced at the disc electrode. This originates from depletion of the electrolyte by NO_3^- reduction at the disc electrode. The presence of the electroactive intermediate products of NO_3^- reduction was not observed in this experiment.

The decrease in current response on the Pt ring electrode for the electrolyte with the addition of NO_2^- shows similar characteristics. A closer look reveals two differences. One is the initial increase in current response on the ring electrode in the potential region of the steep increase in NO_2^- reduction current. This behaviour corresponds to the formation of another electroactive intermediate product in this potential range sensitive to the oxidation on the Pt anode. This results in an increase in the anodic current response at the Pt ring electrode.

We do not have a satisfactory explanation for the second feature, the decrease in current during the reverse potential sweep. This feature appears clearly on the response curves measured for the Cu electrode only. This indicates that products of NO_2^- reduction at the Cu disc electrode transferred to the Pt ring electrode may cause inhibition of catalytic activity. This explanation also applies to the cathodic current response on the ring electrode for the Cu cathode with the addition of Cu ions to the electrolyte (Figure 5). Cathodic current originates from the inhibition of the hydrogen oxidation reaction on the ring electrode by the NH_3 evolved in this potential range on the disc electrode. This inhibition does not take place in the blank experiment. Therefore, after subtraction of the blank experiment from the response obtained for NO_3^- addition, the resulting curve enters the cathodic region. Indirect evidence for such behaviour is the decrease in oxygen evolution current density on the Pt electrode after addition of 0.4 g dm^{-3} of NH_3 to the electrolyte.

The constant current batch electrolysis results confirm the conclusions made using cyclic voltammetry. The Cu electrode demonstrated high electrocatalytic activity for NO_3^- reduction. At 4 mA cm^{-2} the NO_3^- concentration, however, did not tend to zero with time, but showed a limiting value of about 50 mg dm^{-3}. The mass transfer phenomenon has to be taken into account. For laminar flow in an empty channel ($v = 4.5 \times 10^{-3}$ m s^{-1}), the mass transfer coefficients k for the plate electrode cell can be evaluated using Equation 1 [15]:

$$Sh = 1.85\left(\frac{d_e}{l} Re\, Sc\right)^{1/3} \quad (1)$$

where d_e, l, Re and Sc are the equivalent flow-through channel diameter, length of the channel, Reynolds and Schmidt numbers, respectively. A value of $k = 3.4 \times 10^{-6}$ m s^{-1} was obtained. The diffusion coefficients were approximated by their values in water $D_{NO_3} = 1.9 \times 10^{-9}$ m^2 s^{-1}, $D_{O_2} = 2.3 \times 10^{-9}$ m^2 s^{-1} [16]. Solution viscosity of 1 M $NaHCO_3$ $\nu' = 1.193 \times 10^{-6}$ m^2 s^{-1} was considered. Assuming NO_3^- reduction proceeds according to Equation 2 and NO_3^- concentration 1 g dm^{-3}, this corresponds to a limiting current density of 4.2 mA cm^{-2}. The limiting current density for the oxygen reduction was evaluated in a similar way. It is approximately two orders of magnitude lower and can be neglected.

$$NO_3^- + 6\,H_2O + 8\,e^- = NH_3 + 9\,OH^- \quad (2)$$

This indicates that electrolysis starts in the region of limiting current. With the decreasing NO_3^- concentration the limiting current is exceeded shortly after the start of electrolysis. This results in a shift in Cu potential to more cathodic values and to the commencement of hydrogen evolution. This causes gradual inactivation of the cathode surface and, after a certain time, leads to complete cessation of NO_3^- reduction. It can be assumed that, with increasing current density under otherwise constant experimental conditions, the limiting concentration of NO_3^- in the solution will increase and vice versa.

5. Conclusions

Cyclic voltammetry has proved to be an efficient tool for testing the electrocatalytic activity of electrode materials

for nitrate reduction in weakly alkaline solutions of sodium bicarbonate. Among the materials studied the copper electrode proved to have the highest catalytic activity. Nitrate reduction using this electrode proceeds via reduction to nitrite as an intermediate product to ammonia as a final product. Lower electrocatalytic activity was also observed for the Ni, graphite and Pt electrodes. Whereas Ni shows behaviour in many aspects similar to Cu, the polarization curves for graphite and Pt, together with the ring electrode responses, indicates a different reduction mechanism and electrocatalytic selectivity.

The main problem is the production of ammonia. Since we are dealing with the regeneration solution and not directly with the treated water, ammonia production does not influence the quality of the treated water. However, ammonia escaping from the solution into the atmosphere is of environmental concern. Further study is necessary to improve the cathode material selectivity towards nitrogen to minimize or eliminate ammonia production.

Acknowledgement

Financial support of this research by the Grant Agency of the Czech Republic under project numbers 104/99/0433 and 104/00/P016 is gratefully acknowledged.

References

1. Council Directive 98/83/EC, 'On the Quality of Water Intended for Human Consumption' (3 Nov. 1998).
2. O.A. Petrii and T.Y. Safonova, *J. Electroanal. Chem.* **331** (1992) 897.
3. S. Ureta-Zanartu and C. Yanez, *Electrochim. Acta* **42** (1997) 1725.
4. J.F.E. Gootzen, P.G.J.M. Peeters, J.M.B. Dukers, L. Lefferts, W. Visscher and J.A.R. Veen, *J. Electroanal. Chem.* **434** (1997) 171.
5. T. Ohmori, M.S. El-Deab and M. Osawa, *J. Electroanal. Chem.* **470** (1999) 46.
6. J.D. Genders, D. Hartsough and D.T. Hobbs, *J. Appl. Electrochem.* **26** (1996) 1.
7. J.O'M. Bockris and J. Kim, *J. Appl. Electrochem.* **27** (1997) 623.
8. J.O'M. Bockris and J. Kim, *J. Electrochem. Soc.* **143** (1996) 3801.
9. H.-L. Li, D.H. Robertson, J.Q. Chambers and D.T. Hobbs, *J. Electrochem. Soc.* **135** (1988) 1154.
10. L. Ma, H.-L. Li and C.-L. Cai, *Electrochim. Acta* **38** (1993) 2773.
11. S. Cattarin, *J. Appl. Electrochem.* **22** (1992) 1077.
12. N. Chebotareva and T. Nyokong, *J. Appl. Electrochem.* **27** (1997) 975.
13. M. Paidar, I. Roušar and K. Bouzek, *J. Appl. Electrochem.* **29** (1999) 611.
14. M. Malát, 'Inorganic Absorption Photometry' (Academia, Prague, 1973) (in Czech).
15. I. Roušar, J. Hostomský, V. Cezner and B. Štverák, *J. Electrochem. Soc.* **118** (1971) 881.
16. P. Pitter, 'Hydrochemie' (SNTL, Prague, 1998) (in Czech).